Single-phase elastic metamaterials for wave filtering

Vasconcelos, Ana C.A.; Schott, Dingena; Aragon, Alejandro M.; Jovanova, Jovana

DOI
10.1115/SMASIS2021-68283

Publication date
2021

Document Version
Final published version

Published in
Proceedings of ASME 2021 Conference on Smart Materials, Adaptive Structures and Intelligent Systems, SMASIS 2021

Citation (APA)
Vasconcelos, A. C. A., Schott, D., Aragon, A. M., & Jovanova, J. (2021). Single-phase elastic metamaterials for wave filtering. In *Proceedings of ASME 2021 Conference on Smart Materials, Adaptive Structures and Intelligent Systems, SMASIS 2021* Article V001T01A015 ASME. https://doi.org/10.1115/SMASIS2021-68283

Proceedings of the ASME 2021 Conference on Smart Materials, Adaptive Structures and Intelligent Systems
SMASIS2021
September 14-15, 2021, Virtual, Online

SMASIS2021-68283

SINGLE-PHASE ELASTIC METAMATERIALS FOR WAVE FILTERING

Ana C. A. Vasconcelos*
Department of Maritime and Transport Technology
Faculty of Mechanical, Maritime and Materials Engineering
Delft University of Technology
Delft, South Holland 2628 CD
The Netherlands
A.C.AzevedoVasconcelos@tudelft.nl

Dingena Schott
Department of Maritime and Transport Technology
Faculty of Mechanical, Maritime and Materials Engineering
Delft University of Technology
Delft, South Holland 2628 CD
The Netherlands
D.L.Schott@tudelft.nl

Alejandro M. Aragón
Department of Precision and Microsystems Engineering
Faculty of Mechanical, Maritime and Materials Engineering
Delft University of Technology
Delft, South Holland 2628 CD
The Netherlands
A.M.Aragon@tudelft.nl

Jovana Jovanova
Department of Maritime and Transport Technology
Faculty of Mechanical, Maritime and Materials Engineering
Delft University of Technology
Delft, South Holland 2628 CD
The Netherlands
J.Jovanova@tudelft.nl

ABSTRACT

This paper discusses an elastic metamaterial for filtering energy from certain frequencies of an incoming wave. The unit cell, which is composed by a single material, is built to obtain a local resonance band gap. Since Bloch - Floquet's periodic condition is enforced to the unit cell, the dynamic characteristics of the metamaterial is obtained by only evaluating such structure. The attenuation mechanism is guaranteed by visualizing bandwidths in which the wave propagation is prohibited. Such bandwidths, denoted as band gaps, are observed in the band structure diagram of the unit cell and in the transmissibility loss over the metamaterial. The assemble of unit cells with different internal geometries results in a filtering mechanism. The proposed single-phase metamaterial could be applied in structures requiring vibration control for selective frequencies.

Keywords: single-phase elastic metamaterials, wave filtering, elastic wave attenuation

INTRODUCTION

Metamaterials are architected structures that have constitutive properties not commonly found in nature. Instead of molecules composed by atoms connected to each other, metamaterials are constituted by unit cells, also named as meta-atoms, which represent the building block of such structures. By designing specific geometric patterns, some unique properties are enacted, such as acoustic/elastic cloaking, negative refractive index, negative permeability, acoustic imaging and acoustic/elastic absorbers [1, 2].

Several metamaterials have been developed for controlling waves of different nature [3]. In the field of acoustics, the first developed metamaterials, called as phononic crystals, used the

*Address all correspondence to this author.

Bragg scattering effect for manipulating acoustic waves. Such effect is based on destructive interference caused by the interaction of incident and scattered waves. This interference occurs at wavelengths of the same order of the unit cell periodicity. Because of this dependence, controlling low frequency waves is not a straightforward process, since it requires huge phononic crystals. As an attempt to control such waves, Liu *et al.* [4] introduced the concept of locally resonant metamaterials, which consists on including resonators in the metamaterial. The wave control depends on the properties of the resonator, instead of the periodicity of the system, which means that the unit cells can have subwavelength dimensions.

One application of elastic metamaterials is attenuating waves for specific frequency ranges [5]. Such filtering process has been applied by using the principle of negative mass density. Chan *et al.* [6] and Milton and Willis [7] first introduced the negative mass effect. Huang and Sun [8] investigated the mechanism behind the wave attenuation and energy transfer of such concept by analyzing a resonator mass-in-mass system. They found that most of the energy is stored by the internal mass when the excitation frequency is close to the local resonance frequency of the lattice system. The resulting system creates band gaps, also named as stop bands, in which the propagation of elastic waves of any direction is prohibited. Tan *et al.* [9] used the same concept in both single and dual mass-in-mass resonator models. The latter model increases the stop band range by including another internal structure with a different resonance frequency. The negative mass density concept was also evaluated in mass-in-mass systems with a dissipative mechanism [10]. Different from previous works, which only discuss analytical and/or numerical results, Khan *et al.* [11] experimentally studied a mass-in-mass system as a locally resonant elastic metamaterial for attenuation of an impact wave. They showed that dissipative elastic metamaterials are a potential mechanism for increasing the band gap width, although the effectiveness of the resonant effect is reduced in comparison with non-dissipative systems.

The filtering effect has been obtained by using mass-in-mass dissipative systems containing one or more internal resonators. However, the local resonance in such systems is reached by combining different materials, which shows a complex issue regarding to the manufacturing process. Furthermore, such systems do not explore the influence of their internal geometry on the band gap formation.

This work proposes an elastic metamaterial for filtering waves for specific frequencies, as shown in Fig. 1. The mechanism behind such design is similar to a mass-in-mass system. However, instead of using multiple materials representing each component, we design a structure made of a single material. Such structure is composed by internal structures whose geometric parameters are chosen to perform similarly to a mass-in-mass system. The stop band average frequency is defined by geometric parameters, which allows tailoring the metamaterial for different

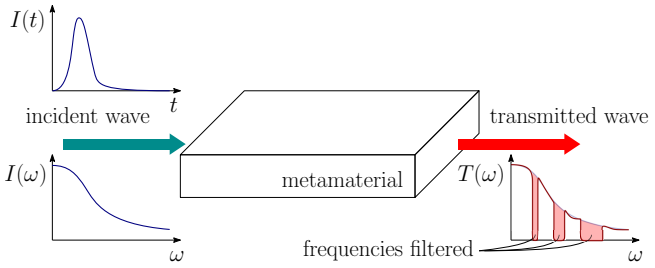

FIGURE 1. CONCEPT OF A METAMATERIAL FOR FILTERING WAVES.

applications. Finite Element Analysis (FEA) is used to obtain the band structure and the transmissibility of the elastic metamaterial. A series of numerical simulations is conducted to evaluate the wave filtering behavior both in frequency and time domains. The findings of this work contribute to develop new passive vibration and noise control structures by using less complex manufacturing processes.

MODEL DESCRIPTION AND METHODS

The metamaterial proposed in this paper consists on an array of periodic unit cells (PUC), whose internal geometry is defined in order to obtain the local resonant mechanism (Fig. 2). The external shape of the PUC is a square of size a with a central hole of radius R_1. The resonator corresponds to an inner mass of radius R_2 connected to the square by means of four beams with width t_b. The paths connector have width t_p. Dimension d denotes the distance between the center of the inner mass and the beams. The unit cell behaves as a conventional mass-in-mass system. As we are interested in single-phase metamaterials, the entire system is constituted of aluminum (Young's modulus E = 70 GPa, density ρ = 2700 kg/m^3 and Poisson's ratio ν = 0.33). No damping is considered in the system.

Since the unit cell is symmetric in both directions, its dynamic characteristics are obtained by using the Irreducible Brillouin Zone (IBZ), which is indicated by the gray triangle in Fig. 2. The unit cell's edges are enforced by periodic boundary conditions according to the following equation of Bloch-Floquet theory,

$$\mathbf{u}(\mathbf{x}+\mathbf{r}) = \mathbf{u}(\mathbf{x})e^{i\,(\mathbf{k}'\cdot\mathbf{r}-\omega t)}, \tag{1}$$

where $\mathbf{x}$ is the position vector, ω is the frequency, $\mathbf{k}' = k'_x\mathbf{i}+k'_y\mathbf{j}$ is the wave vector and $\mathbf{r}$ denotes the spatial periodicity, respectively. The band structure diagram is obtained by solving the dispersion relation of the propagating waves, which defines the relation between the wave vector and the frequency of the propagating wave. Two techniques can be applied for solving such

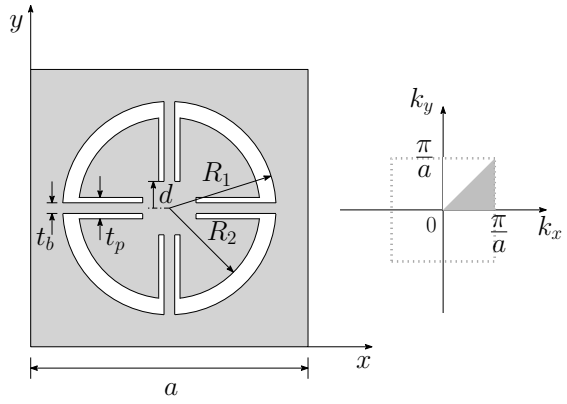

FIGURE 2. SINGLE MATERIAL UNIT CELL REPRESENTATION AND CORRESPONDING IRREDUCIBLE BRILLOUIN ZONE.

relation: the $\mathbf{k}'(\omega)$ and $\omega(\mathbf{k}')$ approaches. In the former, frequencies are imposed in the system and the wave vectors, which can be a complex value, are obtained. The imaginary part of such vector quantifies the wave attenuation. In the latter, the frequencies are obtained by imposing real-value wave vectors defined by the IBZ. In this paper, the second approach is performed in the commercial software COMSOL Multiphysics™.

Another analysis for evaluating the band gap is through the transmissibility diagram. This method calculates the ratio between the output and input displacements in a system due to a harmonic signal. In the metamaterial, this ratio corresponds to the analysis of a point before and after the array of unit cells, respectively. The transmission relation T is calculated as follows

$$T = 20\log\left(\frac{u_N}{u_0}\right) \tag{2}$$

where u_0 and u_N denote the total displacement in the points p_i and p_o, respectively, located at the array of N unit cells, as shown in Fig. 3.

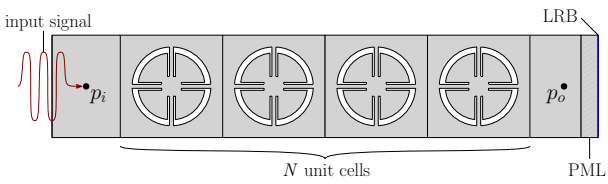

FIGURE 3. ARRAY OF N UNIT CELLS USED FOR TRANSMISSION ANALYSIS.

In order to evaluate the filtering effect through the array of unit cells, a transient analysis is also performed. For such analysis, a longitudinal wave with maximum amplitude F_{max} is considered.

Since we are not interested in wave reflection, an infinite domain need to be enforced by using the Perfectly Matched Layer (PML) and low-reflecting boundary (LRB) condition. The LRB condition absorbs waves that propagate perpendicularly to the boundary and the PML is used for improving such absorption.

NUMERICAL RESULTS

In order to investigate the filtering mechanism of the proposed metamaterial, the band structure and the transmission diagrams previously described are discussed. As a first investigation, only longitudinal waves propagating along the x-direction are assumed. Because of that, partial band gaps, which represent the attenuation of waves of specific directions, are enough for these analyses. The geometrical properties that influence the partial band gaps are also discussed.

Band Structure Diagram and Transmission Analysis

The band structure diagram is obtained by using the $\omega(\mathbf{k}')$ approach. Only the horizontal path of the IBZ needs to be evaluated ($0 \leq k_x \leq \pi/a$ and $k_y = 0$), since the propagating waves are of longitudinal type.

In dynamics, it is well known that the resonance frequencies of a structure depend on its stiffness and mass. Since the band gap due to the locally resonant effect is related to such frequencies, the parameters on the inner geometry and the beam connectors require attention, as they represent the mass and stiffness of the unit cell's resonator. In this section, three parametric analyses are discussed: increase of the inner mass radius, decrease of the width of the beams connecting the outer structure to the inner mass, and the number of connectors. As only the properties of the beams and the inner mass, t_b and R_2, is taken into account, the other dimensions are kept constant. The values of the fixed dimensions are a = 100 mm, t_p = 10 mm, d = 10 mm and R_1 = 40 mm. The thickness of the unit cell is 1 mm. In the following results, the wavenumber $\mathbf{k}$ was turned to a nondimensional value by making $\mathbf{k} = (\pi/a)\mathbf{k}'$.

For the transmission analysis, an array of N = 10 unit cells is studied (Fig. 3). The structure is excited at the left end with a harmonic horizontal displacement signal of amplitude 0.1 mm. PML and LRB are imposed at the right end. The remaining edges are traction-free.

Both diagrams are analyzed for frequencies from 0 Hz to 6000 Hz, since the resonance frequencies of the proposed resonators are contained in this range. The shaded regions in the band structure and transmission diagrams presented below are the partial band gaps. It is worth noting that the colored curves in the band structure diagrams represent each eigenfrequency as a function of the wavenumber. The focus on these diagrams is to

highlight the partial band gaps.

Variation of inner mass radius R_2 In this study, the mass of the resonator from the proposed unit cell is varied by modifying the radius of the inner circle R_2 shown in Fig. 2.

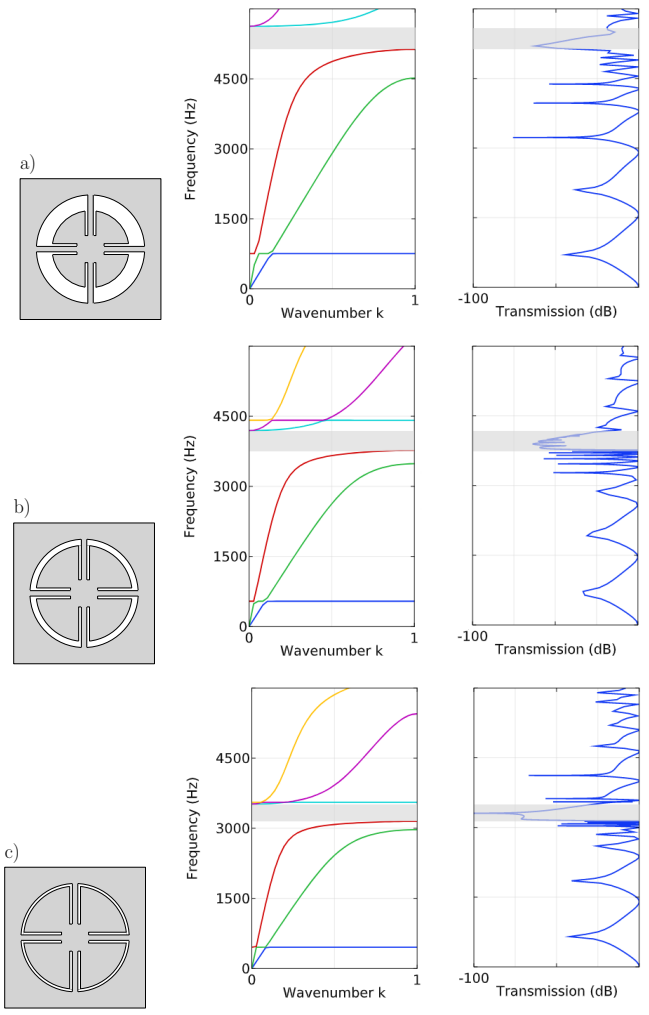

FIGURE 4. BAND STRUCTURE AND TRANSMISSION DIAGRAMS OF UNIT CELLS WITH INNER RADIUS: a) R_2 = 30 mm, b) R_2 = 35 mm AND c) R_2 = 38 mm.

Figure 4 shows the variation of the band structure (middle column) and transmission (right column) diagrams with the increase of the radius R_2. From the band diagrams, we notice that a partial band gap is obtained in all cases. As the radius R_2 increases from 30 mm to 38 mm, the central frequency of the partial band gap decreases from about 3900 Hz (Fig. 4b) to 3250 Hz (Fig. 4c) as well as its bandwidth reduces. Such phenomenon occurs because of the increase of the mass contribution in the unit cell. The wave filtering is also obtained in the transmission diagram, where a reduction of transmission after the array of unit cells is identified by the several peaks in the bandwidths corresponding to the gaps from the band structure. By only increasing their inner mass, such unit cells can be applied for filtering high frequency waves.

Variation of beam width t_b In this study, the influence of the beam's width over the dynamic characteristics of the unit cell is discussed. The inner mass radius is R_2 = 35 mm.

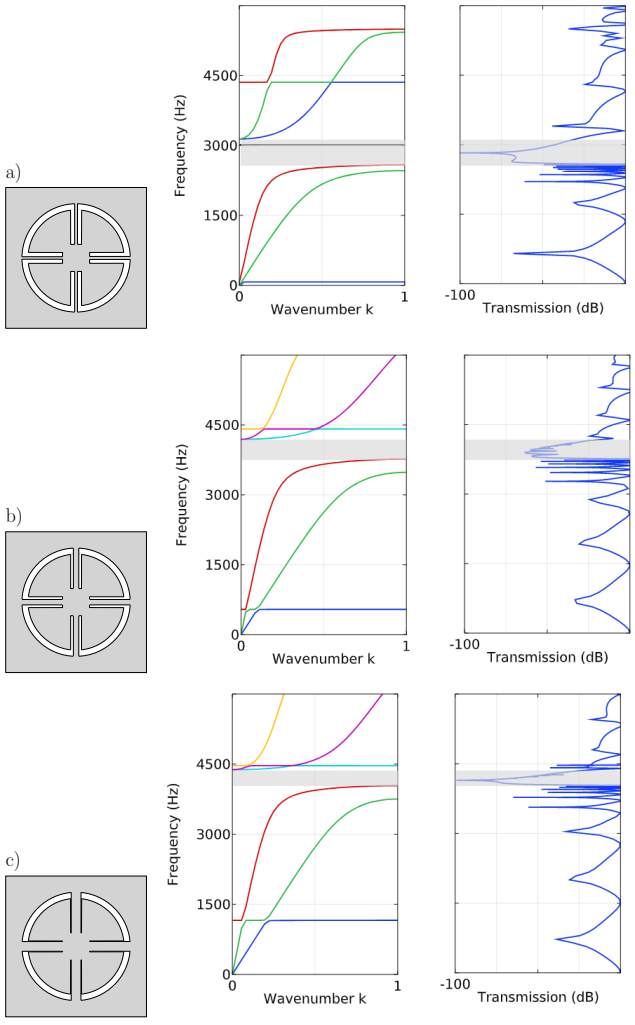

FIGURE 5. BAND STRUCTURE AND TRANSMISSION DIAGRAMS OF UNIT CELLS WITH BEAM WIDTH: a) t_b = 0.5 mm, b) t_b = 2 mm AND c) t_b = 3.5 mm.

Figure 5 presents how the beam's width is related to the frequencies in which waves are attenuated by the filter. Notice from the band structures that by increasing the width t_b from 0.5 mm to 3.5 mm, the central frequency of the partial stop band moves from 2750 Hz for thinner beams (Fig. 5a) to 4250 Hz for thicker beams (Fig. 5c) and the bandwidth becomes narrower. This reduction occurs because the stiffness of the the beams is proportional to their width. Hence, this effect increases the resonator's stiffness. The same partial band gaps are presented in the transmission diagram, where we can see a high reduction of the wave propagation. As in the previous parametric analysis, the unit cells presented here can also be used for high frequency wave filtering by only adjusting the beam's width.

Variation of number of beam connectors Another important analysis is the evaluation of the band diagram when the number of beam connecting the inner mass to the outer structure is reduced. Fig. 6 shows one remarkable characteristic from such unit cell. By removing the two horizontal beams, the stiffness of the overall unit cell is drastically reduced, which results in low eigenfrequency values. Also, we can observe a reduction in bandwidth of the partial band gap, in which a central frequency of about 360 Hz is obtained.

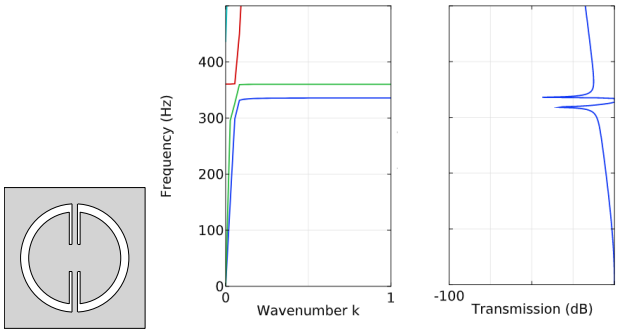

FIGURE 6. BAND STRUCTURE AND TRANSMISSION DIAGRAMS OF UNIT CELL WITH TWO BEAMS OF WIDTH t_b = 2 mm.

Here, the case of low frequency partial band gap is evaluated. From the previous studies, we showed that such band gap is obtained by increasing the mass and decreasing the stiffness of the system, which corresponds to the unit cells illustrated in Fig. 4c and 5a, respectively.

Figure 7 presents those unit cells without the horizontal beams. By comparing Fig. 7a to Fig. 6, we notice a decrease in the resonance frequency from about 350 Hz to 300 Hz. In the transmission diagram, we also observe that the bandwidth becomes narrower. Now, comparing Fig. 7b to Fig. 6, it is noted

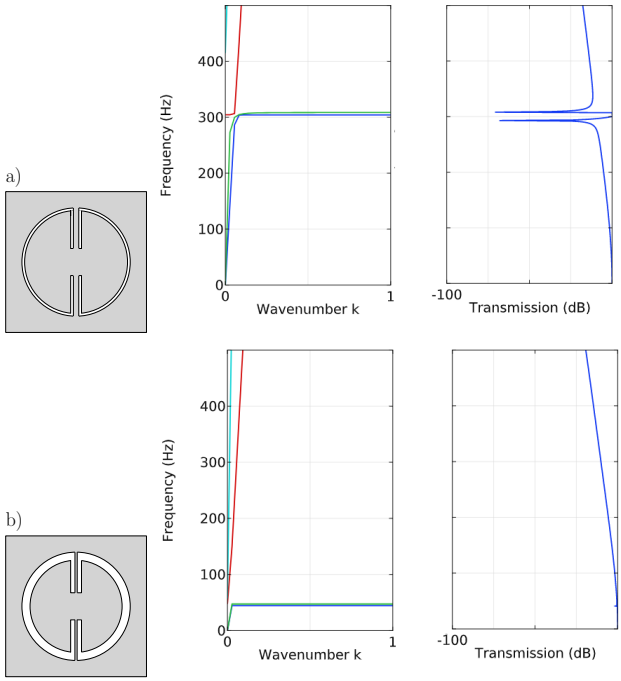

FIGURE 7. BAND STRUCTURE AND TRANSMISSION DIAGRAMS OF UNIT CELLS FROM a) FIG. 4c AND b) FIG. 5a WITHOUT HORIZONTAL BEAMS.

that the eigenfrequencies for the unit cells with thinner beams are quite low. However, we cannot identify any partial band gap for such case, since no reduction of transmission is observed in the right figure. Although, these unit cells can be employed for filtering low frequency waves.

In order to obtain a metamaterial that is able to filter waves from specific frequencies, a combination of unit cells with different resonators is required. Each resonator is responsible for attenuating the wave in a certain frequency. Fig. 8 shows an array containing two different unit cells distributed along the x-direction. In this analysis, N = 20 unit cells are considered, 10 of them are the one presented in Fig. 5a and the remaining correspond to the one presented in Fig. 6.

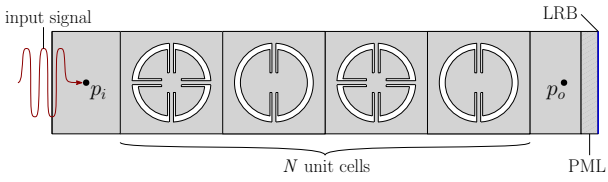

FIGURE 8. ARRAY OF N DIFFERENT UNIT CELLS USED FOR TRANSMISSION ANALYSIS.

Figure 9 presents the transmission diagram for the metamaterial with two different unit cells. It is important to note that the transmission loss in the frequencies corresponding to each type of unit cell (300 Hz and the range between 2600 Hz and 3000 Hz) is also shown for the combined metamaterial. Based on this result, if more resonators with other frequencies are included in the array, more waves corresponded to those frequencies are filtered.

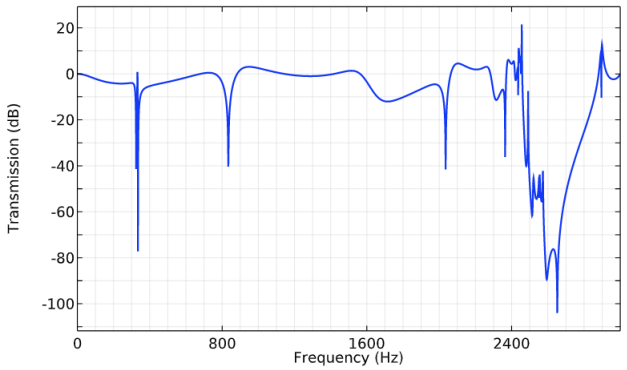

FIGURE 9. TRANSMISSION DIAGRAM OF ARRAY OF UNIT CELLS PRESENTED IN FIG. 8.

CONCLUSIONS

This paper studied an single-phased elastic metamaterial for filtering waves in specific frequencies. Since the resonance properties of the metamaterial depend only on the internal geometry of the unit cell, a sensitivity analysis was performed in the components of the resonator in order to identify the parameters that define the partial band gaps. The analysis showed that the unit cell can be used for filtering high and low frequency waves by adjusting the geometry of the internal mass or the stiffness components (beam dimensions). The combination of unit cells with different resonant frequencies allows the construction of metamaterial-based structures for attenuating waves of low and high frequencies simultaneously, or for improving the bandwidth of the low-frequency band gap. As the metamaterial consists on a single material, the manufacturing process becomes less complex, which makes it a new alternative for passive vibration and noise control in structures.

ACKNOWLEDGMENT

The authors would like to thank Delft University of Technology for enabling this research as cohesion project awarded by the faculty of Mechanical, Maritime and Materials Engineering

REFERENCES

[1] Hussein, M. I., Leamy, M. J., and Ruzzene, M., 2014. "Dynamics of phononic materials and structures: Historical origins, recent progress, and future outlook". *Applied Mechanics Reviews,* ***66***(4).

[2] Jovanova, J., Nastevska, A., and Frecker, M., 2019. "Tailoring energy absorption with functional grading of a contact-aided compliant mechanism". *Smart Materials and Structures,* ***28***(8), p. 084003.

[3] Kadic, M., Milton, G. W., van Hecke, M., and Wegener, M., 2019. "3d metamaterials". *Nature Reviews Physics,* ***1***(3), pp. 198–210.

[4] Liu, Z., Chan, C. T., and Sheng, P., 2005. "Analytic model of phononic crystals with local resonances". *Physical Review B,* ***71***(1), p. 014103.

[5] Zhu, H., and Semperlotti, F., 2013. "Metamaterial based embedded acoustic filters for structural applications". *AIP Advances,* ***3***(9), p. 092121.

[6] Chan, C. T., Li, J., and Fung, K. H., 2006. "On extending the concept of double negativity to acoustic waves". *Journal of Zhejiang University-SCIENCE A,* ***7***(1), pp. 24–28.

[7] Milton, G. W., and Willis, J. R., 2007. "On modifications of newton's second law and linear continuum elastodynamics". *Proceedings of the Royal Society A: Mathematical, Physical and Engineering Sciences,* ***463***(2079), pp. 855–880.

[8] Huang, H., and Sun, C., 2009. "Wave attenuation mechanism in an acoustic metamaterial with negative effective mass density". *New Journal of Physics,* ***11***(1), p. 013003.

[9] Tan, K. T., Huang, H., and Sun, C., 2014. "Blast-wave impact mitigation using negative effective mass density concept of elastic metamaterials". *International Journal of Impact Engineering,* ***64***, pp. 20–29.

[10] Chen, Y., Barnhart, M., Chen, J., Hu, G., Sun, C., and Huang, G., 2016. "Dissipative elastic metamaterials for broadband wave mitigation at subwavelength scale". *Composite Structures,* ***136***, pp. 358–371.

[11] Khan, M., Li, B., and Tan, K., 2018. "Impact load wave transmission in elastic metamaterials". *International Journal of Impact Engineering,* ***118***, pp. 50–59.